PYRAMID SHAPED NANOANTENNA FOR SOLAR ENERGY HARVESTING

Thesis submitted

In partial fulfilment of the requirements for the

Degree of

MASTER OF SCIENCE

in

Physics

by

Akanksha Tyagi

(2K22/MSCPHY/59)

Lakshay Sharma

(2k22/MSCPHY/23)

Under the supervision of

Dr. Kamal Kishor

(Delhi Technological University)

To the

Department of Applied Physics

DELHI TECHNOLOGICAL UNIVERSITY

(Formerly Delhi College of Engineering)

Shahbad Daulatpur, Main Bawana Road, Delhi-110042

May,2024

DELHI TECHNOLOGICAL UNIVERSITY
(Formerly Delhi College of Engineering)
Shahbad Daulatpur, Main Bawana Road, Delhi-42

ACKNOWLEGMENTS

We would like to express our heartfelt gratitude to our mentors, **Dr. KamalKishor** for their keen interest and valuable guidance throughout the course of this project. Their constructive advice and constant motivation have been instrumental in the completion of our venture. We thank profusely all the teachers and staff of the Department of Applied Physics, DTU for providing us with the opportunity to prepare this project. We also want to express our deep sense of gratitude to **Dr. Monu Nath Baitha** (Yonsei University, South Korea), **Mr. Ankit & Mrs. Ritika Ranga** (Delhi Technological University, Delhi) for valuable guidance throughout the project. We would also like to thank our friends for their constant support and valuable input at critical junctures during the completion of this project.

Akanksha Tyagi
(2K22/MSCPHY/59)

Lakshay Sharma
(2k22/MSCPHY/23)

DELHI TECHNOLOGICAL UNIVERSITY
(Formerly Delhi College of Engineering)
Shahbad Daulatpur, Main Bawana Road, Delhi-42

CANDIDATE'S DECLARATION

We hereby certify that the work, which is presented in the thesis entitled "**Pyramid Shaped Nanoantenna for Solar Energy Harvesting**" in fulfillment of the requirement for the award of the Degree of Master in Science in Physics and submitted to the Department of Applied Physics, Delhi Technological University, Delhi is an authentic record of our own, carried out during a period from January to May 2023, under the supervision of **Dr. Kamal Kishor.**

The work presented in this report has not been submitted and is not under consideration for the award for any other course/degree of this or any other Institute/University.

Akanksha Tyagi **(2K22/MSCPHY/59)**

Lakshay Sharma **(2k22/MSCPHY/23)**

This is to certify that the student has incorporated all corrections suggested by the examiners in thesis and the statement made by the candidate is correct to the best of our knowledge.

Dr. Kamal Kishor
(Supervisor)

Signature of External Examiner

DELHI TECHNOLOGICAL UNIVERSITY
(Formerly Delhi College of Engineering)
Shahbad Daulatpur, Main Bawana Road, Delhi-42

CERTIFICATE BY THE SUPERVISOR

Certified that **Akanksha Tyagi** (2k22/MSCPHY/59) has carried out their search work presented in this thesis entitled "**Pyramid shaped Nanoantenna for Solar Energy Harvesting**" for the award of **Master of Science from Department of Applied Physics, Delhi Technological University, Delhi,** under my supervision. The thesis embodies results of original work, and studies are carried out by the student herself and the contents of the thesis do not form for the award of any other degree to the candidate or to anybody else from this or any other University.

Dr. Kamal Kishor
(Department of Applied Physics)
Delhi Technological University

ABSTRACT

In this research, we present a relative analysis of the Harvesting and radiation efficiency of Pyramid shaped nanoantenna. Geometrical factors of the nanoantenna, such as its height *h*, width *w*, and gap *g*, have been diverse in order to assess their impact on the radiation efficiency and field enhancement. The effect of parametric variations on the gold nanoantenna has been explored, and the results have been reported in terms of radiation efficiency and Harvesting Efficiency.

Keywords: Nanoantenna, Solar Energy, Plasmonic, Efficiency

LIST OF PUBLICATIONS

Title of Paper: Pyramid Shaped Nanoantenna for Solar Energy Harvesting

Author Names: Akanksha Tyagi, Lakshay Sharma, Kamal Kishor

Name of Conference: Recent Advances in Functional Material (RAFM-2024)

Status of Paper (Accepted/Published/Communicated): Communicated

TABLE OF CONTENTS

LIST OF TABLES

LIST OF FIGURES

LIST OF SYMBOLS/ABBREVIATIONS

RF: Radio Frequency

SPR: Surface Plasmon Resonance

SERS: Surface Enhanced Raman Scattering

SPP: Surface Plasmon Polariton

LSPR: Localized Surface Plasmon Resonance

ρ_v**:** Charge Density of time-varying volume

ε**:** Relative Electric permittivity

μ**:** Relative Magnetic permeability

J**:** Electric Current Density

D & B: The flux Densities of the electric and magnetic fields respectively.

E & H: The Intensities of magnetic and electric fields respectively.

ω **:** Radial Frequency

n: Refractive index

k: Wavenumber

F: Directivity

U: Radiation Intensity

η_{rad}: Radiation Efficiency

S_{ab}**:** Power Absorbed by the Nanoantenna

S_{rad}**:** Power Radiated

PML: Perfectly Matched Layer

FEM: Finite Element Technique

PDE: Partial Differential Equations

h: Height of Antenna Arms

w: Width of the Antenna Face

g: Gap between the Two Arms of Antenna

CHAPTER 1
INTRODUCTION

1.1 Introduction

Our solar powerhouse, the sun, is a plentiful supply of energy that has enthralled human civilization for ages. Solar energy, which is produced by the sun's heat and radiation, has become essential for solving today's energy problems. In the mid-to far-infrared wavelength ranges, some solar energy is absorbed by atmospheric gases and reradiated to the earth's surface. Over a broad range, the power density of solar radiation that reaches Earth's atmosphere is around 1370 W/m2. This spectrum may be divided into three primary bands: visible light (400 nm < λ < 700 nm), where the content is roughly 39%; ultraviolet (UV) radiation (λ < 400 nm), of which the content is less than 9%; and infrared (IR) radiation, which makes up the remaining 52%.

The PV solar cell technology is created to collect solar power in the visible range (400–700 nm), which comprises 46% of the solar spectrum[1]. After the first photovoltaic (PV) cell was invented in the beginning of the 1950s, photovoltaic technology has advanced quickly [**Figure 1**]. Unfortunately, due to their poor efficiency, this progress is still unable to meet the market need for solar panels.

"Nano-antennas" are one of the alternate methods to technology, where they outperform the present solar cells in terms of efficiency (theoretically 100%). The idea of employing nano-antennas to harvest solar energy from the sun and earth's radiation basically based on the idea that a nano-antenna experiences an electromagnetic wave incident which cause a current that changes throughout time to be produced on the surface of the antenna, resulting in the generation of a voltage at the antenna's feeding point[2].

Figure 1 Photovoltaic Cell

An antenna's parameters are crucial for both design and measurement in order to assess the antenna's performance. The radiation pattern, gain, efficiency, and bandwidth are typically the antenna parameters of interest. To further confirm that an antenna satisfies the necessary design parameters, the antenna's performance can also be measured. The near field and far field portions of the antenna are measured. To make it easier for researchers to determine the antenna's field dispersion, these two zones have been specified. Some energy is retained in the vicinity of the antenna in the near field region rather than being emitted by the antenna over vast distances. Consequently, the distance from the antenna has a significant impact on the dispersion of the angular field. The rotational field distribution is devoid of this distance, though, because the energy in the far field region is radiated to an infinite distance from the source. The antenna's capability in the far field region is crucial since it is frequently examined for its radiation ability in the realm of radio frequency (RF) or broadband range. The optical antenna, often referred to as a nanoantenna, is an optical light coupling device made of metallic particles with a nanoscale size. Utilizing the quick advancements in nanotechnology and optical materials, optical antennas for harvesting sunlight have drawn a lot of attention since they offer a practical and effective substitute for more conventional energy harvesting technologies like solar panels.

1.2 Literature Survey

The term "nanoantenna" was initially used to describe the resonant properties of nanoparticles as resonators for local field enhancement [3], and it initially appeared to be a novel idea. The resonance induced due to the interaction between light photons and the conduction electrons behavior in metal nanoparticles is called surface plasmon resonance (SPR). By exploiting surface plasmon resonance, the nanoparticles can concentrate and confine visible and near-infrared light into nano meter scale dimensions, producing local enhanced fields of significant magnitude [4]. These metallic nanoparticles have been thoroughly studied [5] and suggested for usage as optical nanoantenna's or plasmonic resonant antennas due to the local field enhancement effects. Surface plasmon resonance-based nanoantenna's are extensively used in near-field sample [6], optical circuits, spectroscopy, surface enhanced Raman scattering (SERS), and optical microscopy or imaging [7].

The nanoantenna designs under investigation now encompass a range of layouts, arrangements, and material constitutions. First off, many material constitutions are used in the nanoantenna designs: Designs made of several materials, such as multi-layered materials and designs filled with a single substance. Gold clearly has the edge over other materials in the optical region when it comes to oxidation resistance when utilized for nanoantenna's. Second, the various combinations of the nanoantenna designs comprise particles with a variety of forms. The forms of sphere , dipole, elliptical pairs, triangles (i.e. bowtie), nanorod, and discs have all been investigated for two coupling particles[8], [9], [10].

The size, structure, and local dielectric atmosphere of nanoparticles have a significant impact on the optical characteristics of nanoantenna's. Nevertheless, these forms were either examined independently or just a small subset of configurations were examined collectively. For reference purposes, the designs of practical nanoantenna's will receive greater attention from researchers.

1.3 Optical Properties of Metals and Surface Plasmon Resonance

We must be aware of a number of novel nanoantenna features in order to comprehend the radiation process of the nanoantenna. The metal films' apertures, the metal-coated fibre probes' apex, and the noble metal nanoparticles with their sharp tips are examples of the field-limiting structures. Depending on their shapes nanoantenna's may create a strong, focused field around them.

Surface plasmons are cumulative excitations of conductive electrons within the metal-dielectric junction caused by electromagnetic radiation. Fields around the structure, in the feed gap, and at the tips may be limited by nanoantenna's, and these fields get smaller the farther we are from the antennas [11]. The nanoantenna's shape, composition, and dielectric background control how strong these limited fields are. The concentration of local fields in nanoantenna's results from surface plasmon resonance. When electromagnetic radiation and surface plasmons interact vigorously, a surface plasmon polariton (SPP) is produced. A long-studied nanoscale phenomenon is localized surface plasmon resonance (LSPR). Strong electromagnetic near-field enhancements and high spectrum absorption and scattering peaks are produced by these resonances, which are linked to noble metal nanostructures. The localized surface plasmon resonance facilitates the operation of the nanoantenna. Strong plasmons produced locally on the nanoparticles are employed as a signal or to boost the fluorescent material's intensity. Silver and gold are typical metals that sustain surface plasmons. However, other metals can also promote surface plasmon production. Numerous spectroscopic measurements, including as fluorescence, Raman scattering, and second harmonic generation, have surface sensitivity which has been improved by the use of surface plasmons. Field confinement provides significant near field amplification, making it useful for various optical applications. Given the radiation function of the nanoantenna, the concepts of antenna theory may be expanded from the RF region to the optical frequencies. It is possible to optimize nanoantenna's to effectively gather electromagnetic energy and restrict it to dimensions smaller than a wavelength.

1.3.1 Electromagnetic Theory

From low frequencies to optical realms, electromagnetic theory is applicable. J. C. Maxwell presented the fundamental ideas of contemporary electromagnetic theory in 1873. He explained the mathematical formulas used to explain several processes, including scattering, reflection, and propagation. Heinrich Hertz established the path for the development of several technologies, including broadcasting, television, radar for detection, antennas, wireless communication, and many more, in 1891 by empirically validating Maxwell's hypothesis.

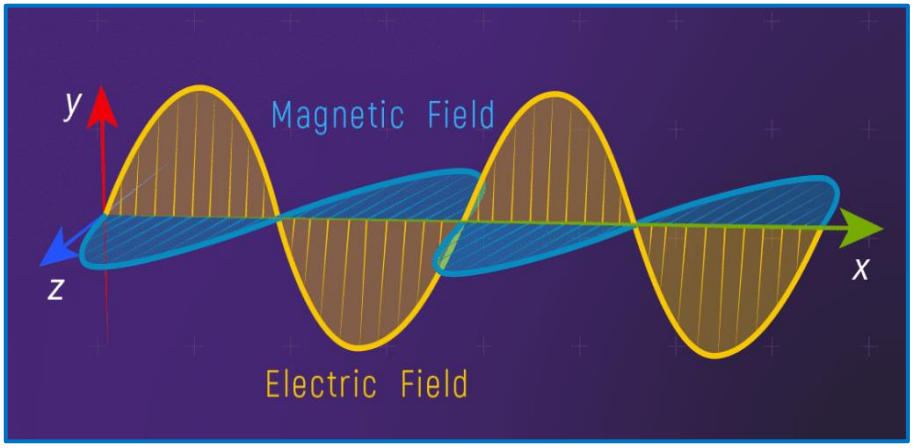

Figure 2 Electromagnetic Wave

1.3.2 Maxwell's equation

The physical phenomenon known as the electromagnetic field, which is a representation of the interplay between the magnetic and electric fields [**Figure 2**], is created in vacuum as electric charges change over duration. As opposed to static charges, which in space will only produce static electric fields. The time-dependent electric field produced by the magnetic fields is one of the causes of time-dependent electric charges. This is described by four differential equations that express the time-dependent Maxwell's equations.

$$\nabla . E = \frac{\rho_v}{\varepsilon} \quad (1)$$

$$\nabla . B = 0 \quad (2)$$

$$\nabla \times E = -\mu \frac{\partial H}{\partial t} \quad (3)$$

$$\nabla \times B = J(t) + \varepsilon \frac{\partial E}{\partial t} \quad (4)$$

Here, $\boldsymbol{\rho_v}$ is charge density of time-varying volume

$\boldsymbol{\varepsilon}$ is Relative Electric permittivity

$\boldsymbol{\mu}$ is Relative Magnetic permeability

$\boldsymbol{J}$ is Electric current density in a material that varies over time

D & B is the flux densities of the electric and magnetic fields, respectively.

E & H is the intensity of magnetic and electric fields that change over time, respectively.

In 1865, James Maxwell created these equations, explaining that electromagnetic radiation is produced by magnetic fields and oscillating electric fields and that the speed of these radiations is equal to the speed of light in empty space. The curl of Eqn. (3) and Eqn. (4) can be used to explain electromagnetic wave propagation equally well. Two key elements, usually referred to as constitutive parameters, impact the features and behavior of an electromagnetic wave in a material in addition to conductivity. They are magnetic permeability and electric permittivity. To put it another way, when combined with the medium's boundary conditions, the aforementioned properties determine the medium's response to an incoming electromagnetic wave. The following two equations represent the relationships between the electric and magnetic field variables in an elementary linear and isotropic medium.

$$D = \varepsilon E \quad (5)$$

$$B = \mu H \quad (6)$$

In Eq. (5) and (6), each is often complex and frequency-based in a lossy dispersive medium and the real quantity isn't in the lossless isotropic medium. Refractive index, n,

and wavenumber k are some significant parameters that can be calculated using Eq. (1) - (6), which are provided as

$$k = \omega\sqrt{\mu\varepsilon} \tag{7}$$

$$\eta = \sqrt{\mu\varepsilon} \tag{8}$$

$$n = \sqrt{\mu_r\varepsilon_r} \tag{9}$$

Were, $\omega = 2\pi f$ defines radial frequency (in rad/sec), f is the frequency in Hz

$\mu_r = \frac{\mu}{\mu_0}$, $\varepsilon_r = \frac{\varepsilon}{\varepsilon_0}$

1.3.3 Wave equations

1st order differential problems, which are coupled in Maxwell's equations, are highly challenging to solve in boundary-value situations. The unknown magnetic and electrical fields are both included in the same equation in linked differential equations. As a result, these equations must be separated and reduced to a single unknown; nonetheless, doing so will raise the order. The wave equation, a 2nd order differential problem that will help with the situation, will be the outcome. The first two of Maxwell's equations provide the wave equation for a conventional, identical, and isotropic medium.

$$\nabla \times E = -\frac{\partial B}{\partial t} \tag{10}$$

$$\nabla \times H = \frac{\partial D}{\partial t} + J \tag{11}$$

Either the magnetic or the electric field must be considered as an unknown in an equation. To do this, take the curl of each of the two sides of (eqn. 10). This results in:

$$\nabla \times \nabla \times E = -\frac{\partial(\nabla \times B)}{\partial t} \tag{12}$$

After replacing (eqn.11) in (eqn.12) and substituting $J = 0$ in (eqn.11) and $B = \mu H$ in (eqn.12), the result is:

$$\nabla \times \nabla \times E = -\mu\varepsilon \frac{\partial^2 E}{\partial t^2} \tag{13}$$

Using the vector identity,

$$\nabla \times \nabla \times F = \nabla(\nabla \cdot F) - \nabla^2 F \tag{14}$$

into (13) leads to:

$$\nabla(\nabla \cdot E) - \nabla^2 E = -\mu\varepsilon \frac{\partial^2 E}{\partial t^2} \tag{15}$$

By applying $\nabla \cdot E = 0$, (24) will be simplified to

$$\nabla^2 E - \mu\varepsilon \frac{\partial^2 E}{\partial t^2} = 0 \tag{16}$$

The time-dependent wave equation, often known as the Helmholtz equation, is the last equation. Similarly, if we begin the deduction from (eqn.11), we may obtain the wave equation for *H*, which is expressed as

$$\nabla^2 H - \mu\varepsilon \frac{\partial^2 H}{\partial t^2} = 0 \tag{17}$$

CHAPTER 2

METHEDOLOGIES

Some common criteria, such radiation intensity, directivity, radiation efficiency, and harvesting efficiency, which are essential for the construction of an RF antenna, will be briefly discussed in this part in order to explain the performance of a nanoantenna.

2.1 Radiation Intensity, Radiation and Loss Resistance

The power emitted from an antenna per unit solid angle is known as radiation intensity, also known as the antenna power pattern, in a particular direction.
The relationship between the total power and radiation intensity is given by:

$$S_{rad} = \oint_{\delta} U_0 d\delta = \int_0^{2\pi} \int_0^{\pi} U \sin\theta \, d\theta \, d\varphi \tag{18}$$

where $d\delta = \sin\theta \, d\theta \, d\varphi$

An isotropic source's radiation intensity is determined by:

$$U_0 = \frac{S_{rad}}{4\pi} \tag{19}$$

The current distribution in a system consisting of two parallel thin wires with an open end will be sinusoidal due to the standing waves. The apparatus emits electromagnetic waves when the ends are twisted to a distance of x/2 from both ends. When the bending angle is *90* degrees, the radiation is at its strongest. The following describes the present distribution on the bent arms' outermost layer:

$$I(z) = I_0 \sin\left[k\left(\frac{x}{2} - |z|\right)\right] \tag{20}$$

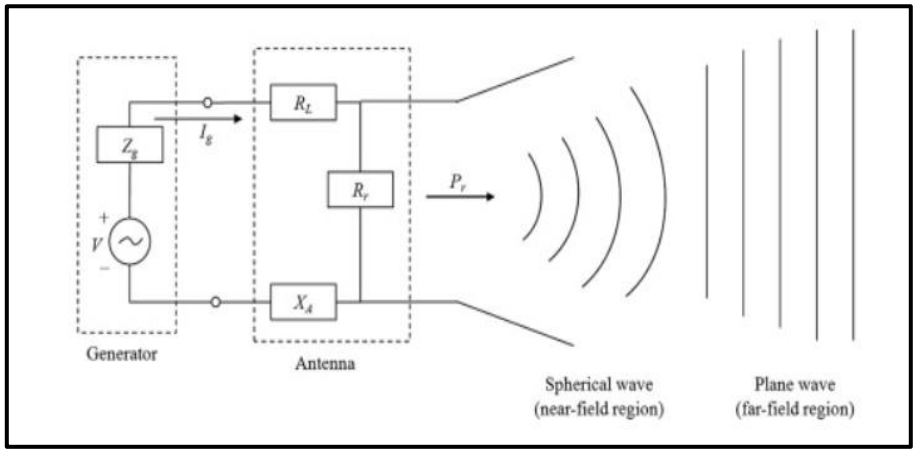

Figure 3 Radiation mechanism of Receiving Antenna

Bending the wire terminals creates a basic dipole antenna with a different impedance, Z_i, than the guiding line's typical impedance, Z_0. Z_i and Z_0's discrepancy would lead us to expect a standing wave pattern. Thus, Input impedance is characterized as the voltage-current ratio at the input antenna terminals.

$$Z_i = R_i + iX_i \tag{21}$$

The true element that constitutes antenna impedance, R_i controls the amount of power lost as heat in an antenna and radiated power, which may be expressed as

$$R_i = R_L + R_r \tag{22}$$

where R_r is the resistance to radiation and R_L is the internal antenna loss resistance. One way to compute the radiated power is to

$$S_r = \frac{R_r I^2}{2} \tag{23}$$

The effectiveness of radiation, η_r, will define as

$$\eta_r = \frac{R_r}{R_r + R_L} \tag{24}$$

In order to accomplish complicated conjugate matching and maximize power transfer, $Z_0 = Z_i^*$. To obtain optimal power transfer, the antenna must be properly matched to the source or guide line. In certain circumstances, the antenna efficiently catches the electromagnetic wave, but just a small portion of electrical power reaches its recipient due to insufficient fitting among the antenna and the resulting circuit.

2.2 Directivity

The term directivity means " the relationship between the radiation intensity coming from the antenna in a particular direction and the average radiation intensity across all directions". The entire power that the antenna emits divided by 4π yields the average radiation intensity. The direction of greatest radiation intensity is assumed if it is not specified explicitly. The directivity of a non-isotropic source F is defined as the proportion of its directionally-directed radiation intensity compared to that from an isotropic source:

$$F = \frac{U}{U_0} = \frac{4\pi U}{S_{rad}} \tag{25}$$

If the radiation's direction is not stated, it suggests the direction of highest intensity of radiation (max. F) as defined by:

$$F_{max} = \frac{U_{max}}{U_0} = \frac{4\pi U_{max}}{S_{rad}} \tag{26}$$

Where, F_{max} represents the maximum directivity

U_0 is the isotropic source's radiation intensity and,

U_{max} is the most radiation intensity.

This indicates that directivity is a metric that represents just the antenna's directional qualities and is thus controlled solely by the pattern.

2.3 Radiation Efficiency

A portion of the light's energy is reradiated and a portion is absorbed by the nanoantenna upon incident light. Radiation efficiency and electric field enhancement are the two main determinants of a nanoantenna's efficacy in solar energy harvesting applications. The proportion of the nanoantenna's strength to the total incident strength is known as the radiation efficiency, and it is represented by the symbol η_{rad} [12]. Mathematically,

$$\eta_{rad} = \frac{S_{rad}}{S_{rad} + S_{ab}} \tag{27}$$

where S_{ab} is the power that the nanoantenna absorbs and S_{rad} is the power that it radiates. By adjusting the nanoantenna's size and, thus, its effective surface area, S_{rad} may be controlled. larger radiation efficiency results from larger effective surface area and better light-gathering capacity of the nanoantenna. Because increased radiation efficiency leads to increased power harvesting, radiation efficiency is important.

2.4 Harvesting Efficiency

The total gathered power is dependent upon both the spectrum's spectral irradiance and radiation efficiency. Thus, by integrating radiation efficiency and Planck's law, the nanoantenna's harvesting efficiency is defined as

$$\eta(total) = \int_0^\infty \frac{S(\lambda)\,\eta(rad\,)d\lambda}{\int_0^\infty S(\lambda)d\lambda} \tag{28}$$

The practical effective power measured intuitively from radiation reaching the nanoantenna is called the harvesting efficiency.

CHAPTER 3
DESIGN AND COMPUTATIONAL DETAILS

3.1 The Fundamental Working Principle

Electromagnetic waves are emitted by hot objects across the electromagnetic spectrum [**Figure 4**]. Temperature affects how much energy is radiated in a certain spectral range. The radiated energy changes more towards shorter wavelengths the hotter the item. An object radiates more energy at longer wavelengths the colder it is. The radiation emitted by a black substance at 6000 K can be used to simulate solar radiation.

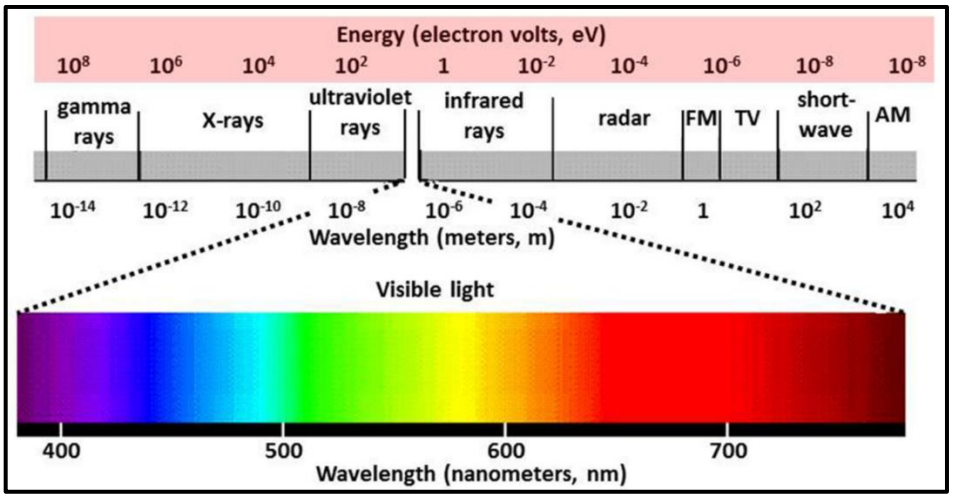

Figure 4 Electromagnetic Spectrum

3.1.1 Planck's Distribution Law: -

Planck's law of black body radiation states that the energy emitted by a dark body as a means of temperature and wavelength is equal to

$$S(\lambda, T) = \frac{2*h*c^2}{\lambda^5} * \frac{1}{\exp\left(\frac{h*c}{\lambda*k*T}\right)-1} \qquad (29)$$

where Planck constant (h) is 6.626 x 10^{-34} Js, and Boltzmann constant (k) is 1.38 x 10^{-23} J/K and T is the dark body's absolute temperature, while λ is its wavelength and light speed

in vacuum (c) is 3 x 10^8 m/sec. The solar spectrum, or normalized intensity vs wavelength curve, is displayed in [**Figure 5**] and was calculated using Planck's law by treating the sun as a dark body with a temperature 6000 k at the surface. Clearly, the highest irradiance is corresponding to the spectral peak, which occurs at about 0.5 x $10^{\wedge-6}$ m.

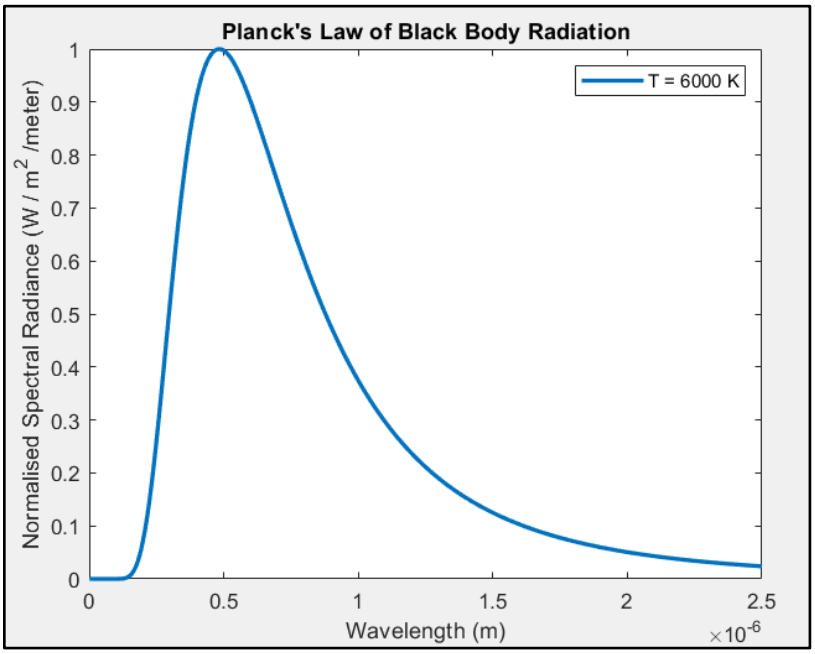

Figure 5 Solar Spectrum

3.1.2 Computational Details:

Numerical simulations are typically used to solve Maxwell's equations and understand the electromagnetic characteristics of antennas. The simulation aims to visualize the distribution of electric fields, allowing for thorough characterization. Predicting these features allows for better resolution of time and space compared to experimentation. Furthermore, these calculations can address specific problems and provide answers to system-related concerns. Numerical simulations may be used to analyze electromagnetic effects, reducing the need for costly tests. Metal distribution at the optical frequency, negative permittivity, losses of energy, and plasmon-polariton impacts from plasmonic nanoantenna's make them difficult to calculate using typical numerical methods. Fine discretization is difficult and time-consuming[13].

Several commercial software packages, including COMSOL MULTIPHYSICS based on FEM, is used to simulate the properties of nanoantenna's in the optical range. The scenarios of metallic wire array, decreased symmetry core shell nanoparticles, and gold elliptic nanoparticle pair array implanted in quartz may all be calculated using COMSOL.

3.2 Design and simulation detail

The design of nanoantenna is structured in a pyramidal shaped. The parameters describing the structure are height, gap, width & the base ratio of the pyramid. The given ***Figure 6*** illustrate the structure.

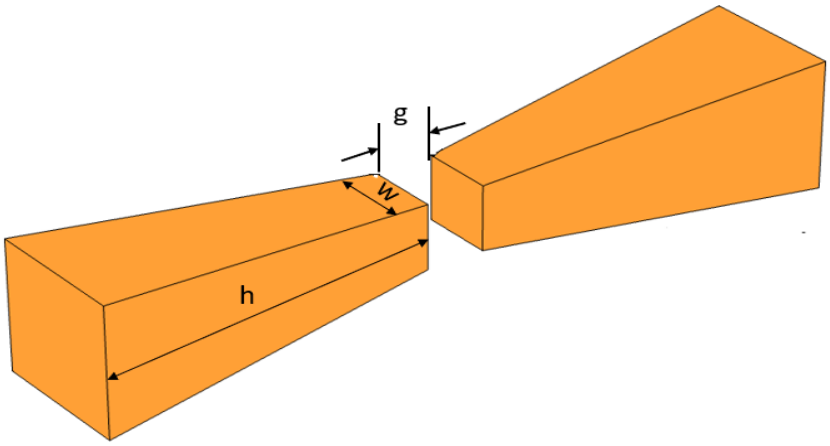

Figure 6 Structure Design of Pyramid Nanoantenna

The Standard parameters value of the proposed structure is 120 nm height (*h*), 10 nm gap (*g*), 50 nm width (*w*) with the base ratio of 0.5. COMSOL Multiphysics was utilized to develop & analyze the suggested nanoantenna using the finite element technique *(FEM)*[13]. An approximative solution to integral and partial differential equations (PDEs) can be found using the FEM technique. The differential equation must be

completely eliminated in order to solve the problem, or it must be converted into an equivalent ordinary differential equation that can be solved by standard methods. The nanoantenna is exposed to plane polarized light with an electric field directed towards its height '*h*'. We have utilized non-uniform meshing in all of the calculations. The PML and the surrounding area have a regular meshing with default element sizes, while the nanoantenna is simulated with an extremely fine meshing. The PML has been maintained at 150 nm in thickness[14]. Since the device & PML thickness & air gap was selected in such a way, increasing any of them further has no effect on the outcomes. The value of gold's permittivity was calculated using experimental data that Johnson & Christy [15] supplied.

CHAPTER 4
GEOMETRY ANALYSIS AND RESULT

4.1 Effect of Height

The primary factor influencing the resonance wavelength is the nanoantenna's height. By adjusting the height *'h'*, the structure may be adjusted to function at various wavelengths. Radiation efficiency & field enhancement have been computed for various nanoantenna sizes in order to investigate the influence of height. In each example, the *'h'* has been adjusted between 115 nm & 125 nm while maintaining a width of 50 nm & a gap of 10 nm.

Figure 7 shows how the field enhancement varies depending on the wavelength at various antenna arm height. As the height increases, the field enhancement peak prominently redshifts. The red shifting of the L*SPR* upon increasing the dimension parallel to the applied electric field is the immediate cause of this. Whereas, **Figure 8** shows the variation between the radiation efficiency & wavelength. The effective surface area that is accessible to receive incoming radiation increases with *'h'*. Therefore, when height rises, radiation efficiency, also known as radiation collection capability, also increases, as **Figure 8** illustrates. Maier (*2007*) presents polarizability in relation to the dielectric constant & particle size, providing a comprehensive explanation of the plasmon resonance of metallic nanoparticles[16] . This suggests that by adjusting the height *'h'*, the nanoantenna may be tailored to a variety of wavelengths.

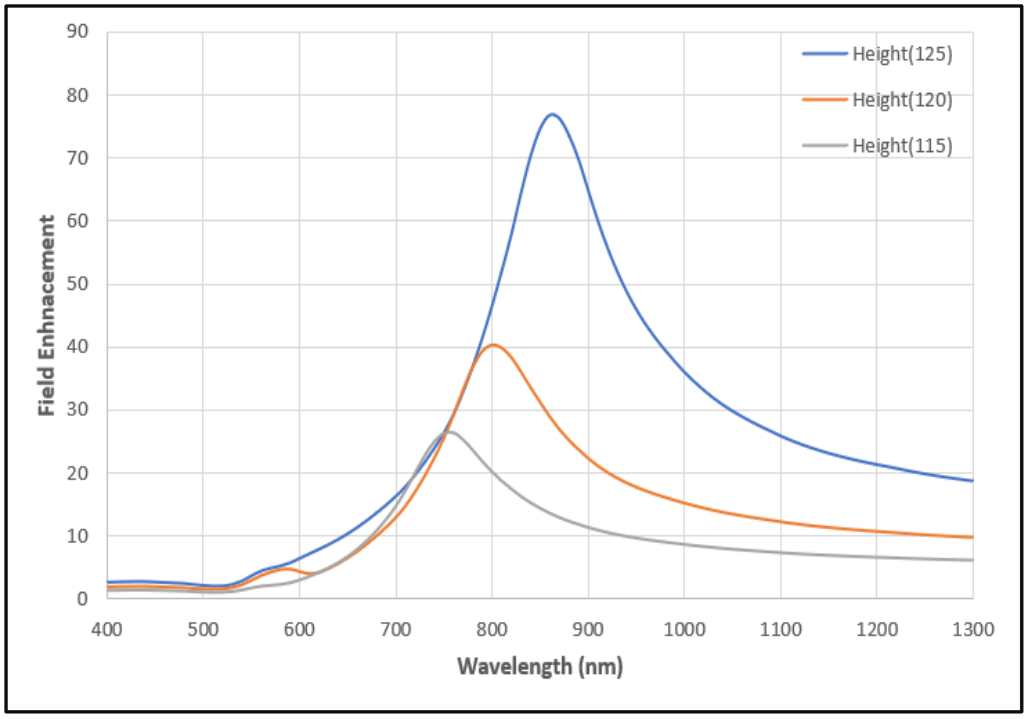

Figure 7 Graph between Field enhancement and Wavelength for variable Height.

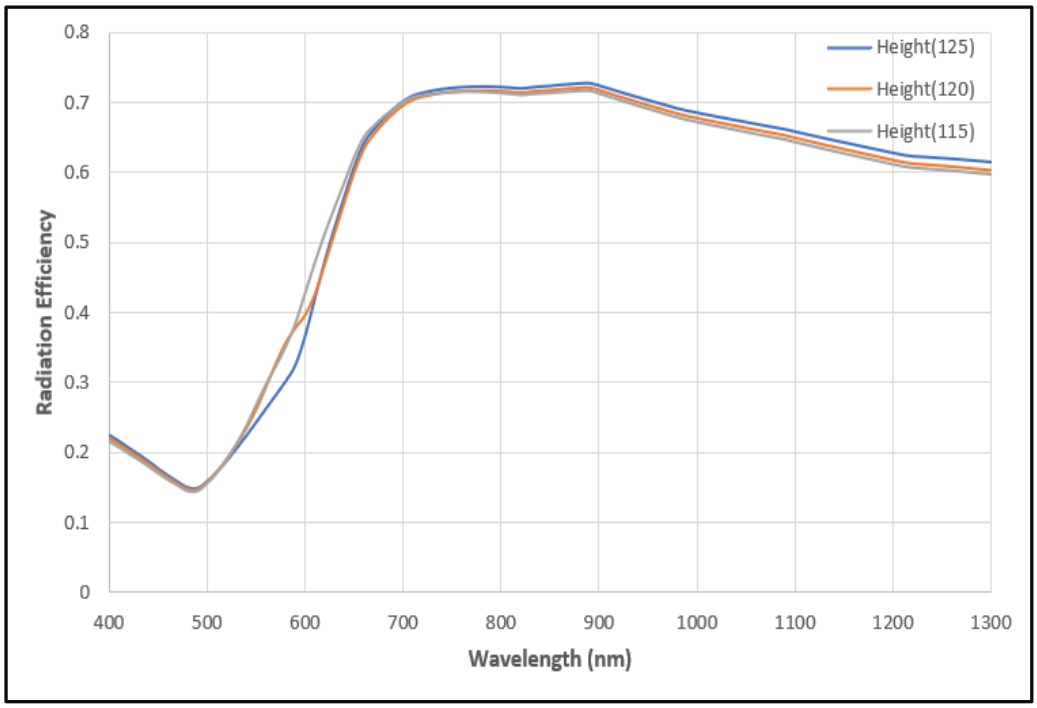

Figure 8 Graph between Radiation Efficiency and Wavelength for variable Height.

Table 1. Harvesting Efficiency to their Corresponding Height (h).

Height (*h*)	***h* (115 nm)**	***h* (120 nm)**	***h* (125 nm)**
Harvesting Efficiency	0.3271	0.3264	0.3257

Table 1 shows the harvesting Efficiency for different heights. Harvesting efficiency is a measure of radiation efficiency, that is the amount of radiation falling on the surface & how much of it is being used. Since the height is increasing the absorbing area increases implying the harvesting efficiency will increase.

4.2 Effect of Width

In addition to height, width is a crucial factor to take into account. Variations in width alter the structure's sharpness, which has an immediate effect on the field's augmentation. Using a range of values—*w* = 10 nm-100 nm, the effect of width has been studied while maintaining a constant *'h'* of 120 nm & *'g'* 10 nm. According to the **Figure 9** & **Figure 10**, at *'w'* 10 nm, the antenna arms get extremely narrow, meaning that the field enhancement is at its highest (*~55*) & the radiation efficiency is at its lowest (*30%*). At *'w'* 100nm, on the other hand, the field enhancement is at its lowest (*~27*) & the radiation efficiency is at its highest (*>80%*). For all other in-between values of *'w'*, the structure remains pyramidal, with the radiation efficiency & field enhancement lying in the region between the two previously described extremes.

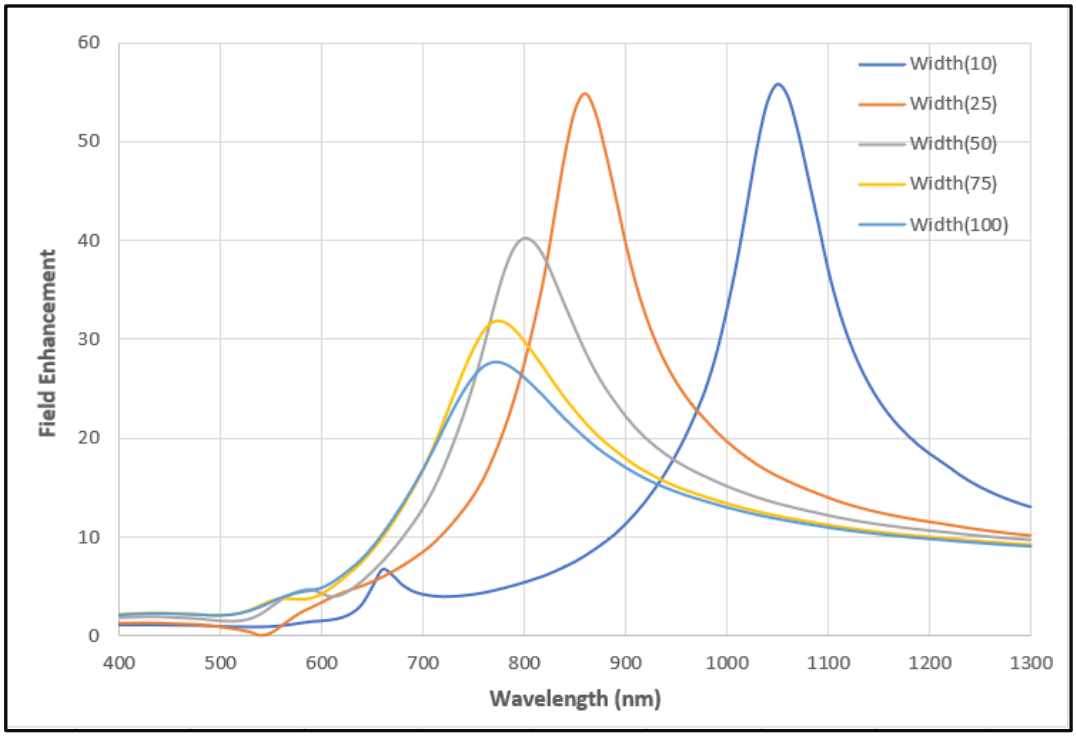

Figure 9 Graph between Field enhancement and Wavelength for variable Width.

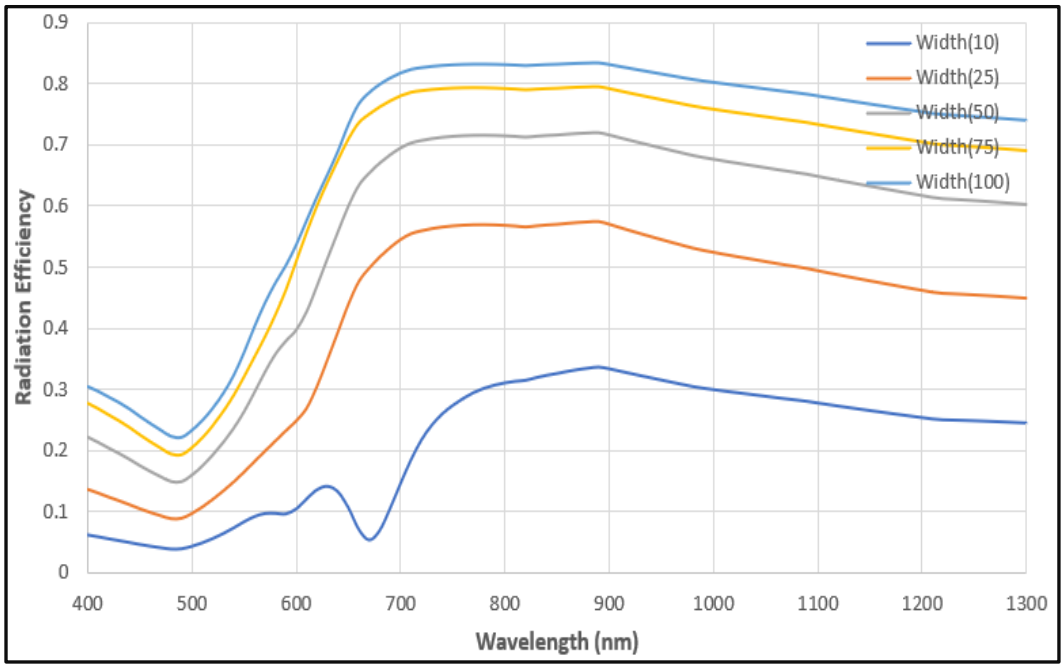

Figure 10 Graph between Radiation Efficiency and Wavelength for variable Width.

This analysis demonstrates the trend whereby radiation efficiency decreases as the width of the nanoantenna is decreased while maintaining a constant height due to a decrease in effective surface area (*as detailed in section 4.1*), however, the arm's increased pointedness results in an increase in field enhancement, or decreased tip angle. Liao and Wokaun have provided a comprehensive discussion of the lightning rod phenomenon, which explains why sharp edges experience near field amplification [17]. Consequently, when the ratio (*h / w*) becomes more slanted, the corners grow sharper, and the field at the point gets better. [17], [18].

Table 2. Harvesting Efficiency to their Corresponding Width (*w*).

Width (*w*)	***w* (10 nm)**	***w* (25 nm)**	***w* (50 nm)**	***w* (75 nm)**	***w* (100 nm)**
Harvesting Efficiency	0.1007	0.2256	0.3264	0.3907	0.4237

Values of harvesting efficiency when width is being Varied from 10 nm to 100 nm can be seen in *Table 2* that on increasing the width harvesting efficiency is increasing. Width face changed from horizontal rectangular faced (at 10 nm) to square (at 50 nm) to vertical rectangular faced (at 100 nm) showing maximum harvesting efficiency at 100 nm.

4.3 Effect of gap

The augmented electric field, whose strength is directly related to gap size which shown in **Figure 11**, is located at the gap *'g'* in-between the antenna arms. Since the localized surface plasmons at the tip surfaces of the two arms overlap more, the resultant field enhancement grows in magnitude as the *'g'* decreases. Nonetheless, the radiation efficiency is essentially unaffected by the variation in gap size since the surface area remains constant. The numerical analysis findings, where *'g'* changes from 5 nm to 20 nm, are displayed in **Figure 12**. On the one hand, it has almost little effect on radiation

efficiency; on the other hand, it significantly reduces field enhancement. This is exactly what was expected based on the previously stated logic.

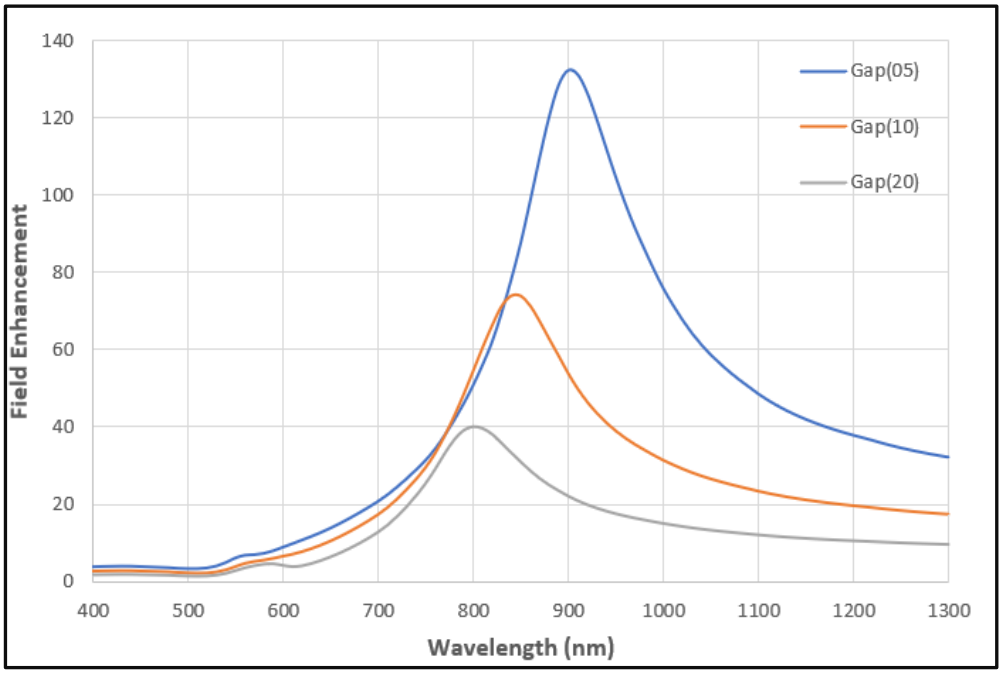

Figure 11 Graph between Field enhancement and Wavelength for variable Gap.

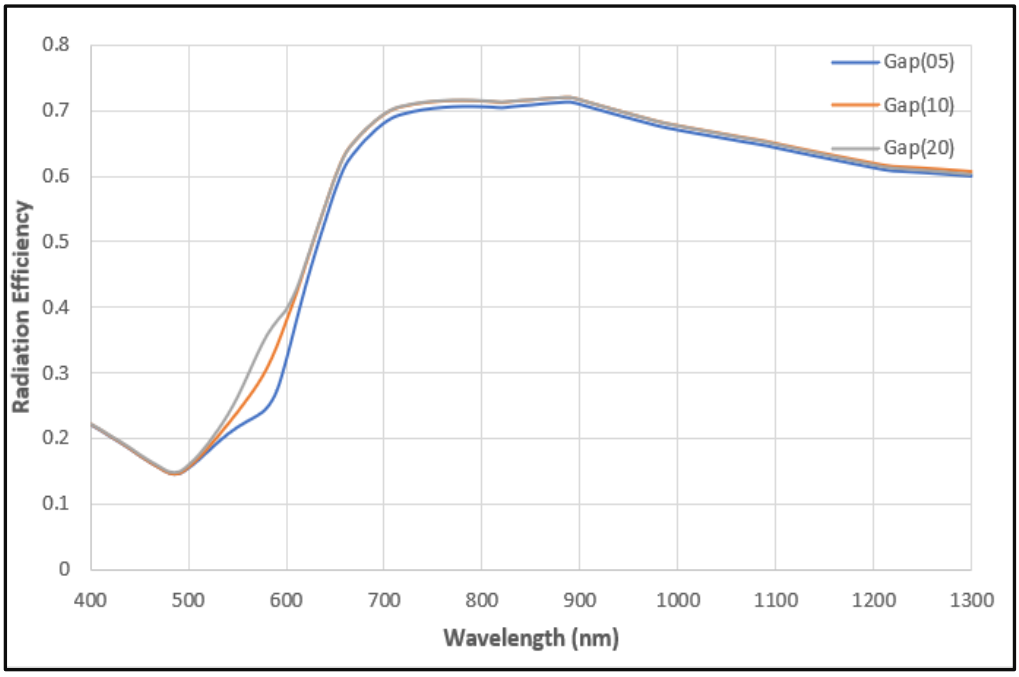

Figure 12 Graph between Radiation Efficiency and Wavelength for variable Gap

Table 3. Harvesting Efficiency to their Corresponding Gap (*g*).

Gap (*g*)	***g* (05 nm)**	***g* (10 nm)**	***g* (20 nm)**
Harvesting Efficiency	0.3112	0.3223	0.3264

Above *Table 3* shows the value of harvesting efficiency on changing the gap but no such change has been measured due to no effect on the surface area of the structure.

CHAPTER 5

CONCLUSION

By adjusting the pyramidal nanoantenna's characteristics, we were able to determine that as the radiation collection capabilities increased, so did the effective surface area that is accessible for receiving incident radiation. On the other hand, when the arm's pointedness improves, the field enhancement rises. Additionally, the observed field enhancement amplitude grows when the localized surface plasmons (LSP) at the tip surfaces of the two arms overlap more.

FIGURE CITATIONS

Figure 1: https://images.app.goo.gl/s3KoNFq1BvWLxpxs5

Figure 2: https://www.online-sciences.com/wp-content/uploads/2015/05/Benefits-of-solar-panels-333-300x178.jpg

Figure 3: https://ars.els-cdn.com/content/image/1-s2.0-B9780124081307000083-f08-13-9780124081307.jpg

Figure 4: https://ozonedepletiontheory.info/wp-content/uploads/2021/04/electromagnetic-spectrum-1-1536x800.jpg

REFERENCE

[1] M. N. Gadalla, M. Abdel-Rahman, and A. Shamim, "Design, Optimization and Fabrication of a 28.3 THz Nano-Rectenna for Infrared Detection and Rectification," *Sci. Rep.*, vol. 4, no. 1, p. 4270, Mar. 2014, doi: 10.1038/srep04270.

[2] M. Hussein, N. F. F. Areed, M. F. O. Hameed, and S. S. A. Obayya, "Design of flower-shaped dipole nano-antenna for energy harvesting," *IET Optoelectron.*, vol. 8, no. 4, pp. 167–173, Aug. 2014, doi: 10.1049/iet-opt.2013.0108.

[3] K. B. Crozier, A. Sundaramurthy, G. S. Kino, and C. F. Quate, "Optical antennas: Resonators for local field enhancement," *J. Appl. Phys.*, vol. 94, no. 7, pp. 4632–4642, Oct. 2003, doi: 10.1063/1.1602956.

[4] P. J. Schuck, D. P. Fromm, A. Sundaramurthy, G. S. Kino, and W. E. Moerner, "Improving the Mismatch between Light and Nanoscale Objects with Gold Bowtie Nanoantennas," *Phys. Rev. Lett.*, vol. 94, no. 1, p. 017402, Jan. 2005, doi: 10.1103/PhysRevLett.94.017402.

[5] E. S. Barnard, J. S. White, A. Chandran, and M. L. Brongersma, "Spectral properties of plasmonic resonator antennas," *Opt. Express*, vol. 16, no. 21, p. 16529, Oct. 2008, doi: 10.1364/OE.16.016529.

[6] S. Kühn, U. Håkanson, L. Rogobete, and V. Sandoghdar, "Enhancement of Single-Molecule Fluorescence Using a Gold Nanoparticle as an Optical Nanoantenna," *Phys. Rev. Lett.*, vol. 97, no. 1, p. 017402, Jul. 2006, doi: 10.1103/PhysRevLett.97.017402.

[7] N. Engheta, "Circuits with Light at Nanoscales: Optical Nanocircuits Inspired by Metamaterials," *Science*, vol. 317, no. 5845, pp. 1698–1702, Sep. 2007, doi: 10.1126/science.1133268.

[8] K. L. Kelly, E. Coronado, L. L. Zhao, and G. C. Schatz, "The Optical Properties of Metal Nanoparticles: The Influence of Size, Shape, and Dielectric Environment," *J. Phys. Chem. B*, vol. 107, no. 3, pp. 668–677, Jan. 2003, doi: 10.1021/jp026731y.

[9] L. Gunnarsson *et al.*, "Confined Plasmons in Nanofabricated Single Silver Particle Pairs: Experimental Observations of Strong Interparticle Interactions," *J. Phys. Chem. B*, vol. 109, no. 3, pp. 1079–1087, Jan. 2005, doi: 10.1021/jp049084e.

[10] A. Sundaramurthy, P. J. Schuck, N. R. Conley, D. P. Fromm, G. S. Kino, and W. E. Moerner, "Toward Nanometer-Scale Optical Photolithography: Utilizing the Near-Field of Bowtie Optical Nanoantennas," *Nano Lett.*, vol. 6, no. 3, pp. 355–360, Mar. 2006, doi: 10.1021/nl052322c.

[11] A. M. A. Sabaawi, "Nanoantennas for Solar Energy Harvesting".

[12] A. M. A. Sabaawi, C. C. Tsimenidis, and B. S. Sharif, "Infra-red spiral nano-antennas," in *2012 Loughborough Antennas & Propagation Conference (LAPC)*, Loughborough, Leicestershire, United Kingdom: IEEE, Nov. 2012, pp. 1–4. doi: 10.1109/LAPC.2012.6403077.

[13] D. W. Pepper and J. C. Heinrich, *The Finite Element Method: Basic Concepts and Applications with MATLAB®, MAPLE, and COMSOL*, 3rd ed. CRC Press, 2017. doi: 10.1201/9781315395104.

[14] R. Ranga, Y. Kalra, and K. Kishor, "Petal shaped nanoantenna for solar energy harvesting," *J. Opt.*, Jan. 2020, doi: 10.1088/2040-8986/ab6ae5.

[15] P. B. Johnson and R. W. Christy, "Optical Constants of the Noble Metals," *Phys. Rev. B*, vol. 6, no. 12, pp. 4370–4379, Dec. 1972, doi: 10.1103/PhysRevB.6.4370.

[16] S. A. Maier, *Plasmonics: fundamentals and applications*. New York: Springer, 2007.

[17] P. F. Liao and A. Wokaun, "Lightning rod effect in surface enhanced Raman scattering," *J. Chem. Phys.*, vol. 76, no. 1, pp. 751–752, Jan. 1982, doi: 10.1063/1.442690.

[18] B. Sturman, E. Podivilov, and M. Gorkunov, "Metal nanoparticles with sharp corners: Universal properties of plasmon resonances," *EPL Europhys. Lett.*, vol. 101, no. 5, p. 57009, Mar. 2013, doi: 10.1209/0295-5075/101/57009.

CONFERENCE CERTIFICATE

ATMA RAM SANATAN DHARMA COLLEGE

UNIVERSITY OF DELHI

Accredited Grade 'A++' By NAAC || All India 6th Rank in NIRF (Ministry of Education)

2nd International Conference on

Recent Advances in Functional Materials (RAFM-2024)

Under the aegis of IQAC and DBT (GoI) star college scheme

Certificate of Oral Presentation

This is to certify that Prof./Dr./Mr./Ms.

AKANKSHA TYAGI & LAKSHAY SHARMA

Delhi Technological University, New Delhi

has presented his/her research work as oral presentation titled

Pyramid Shaped Nanoantenna for Solar Energy Harvesting.

in 2nd International Conference on "Recent Advances in Functional Materials" (RAFM-2024) organised by Department of Physics under the aegis of IQAC ARSD College, University of Delhi & DBT (GoI) Star College during March 14-16, 2024 via online mode.

Dr. Manish Kumar
Convener, RAFM-2024

Prof. Vinita Tuli
Coordinator, IQAC

Prof. Gyantosh Kumar Jha
Principal, ARSD College

Certificate No: ARSD/RAFM-2024/OT/010

SCOPUS INDEX PROOF

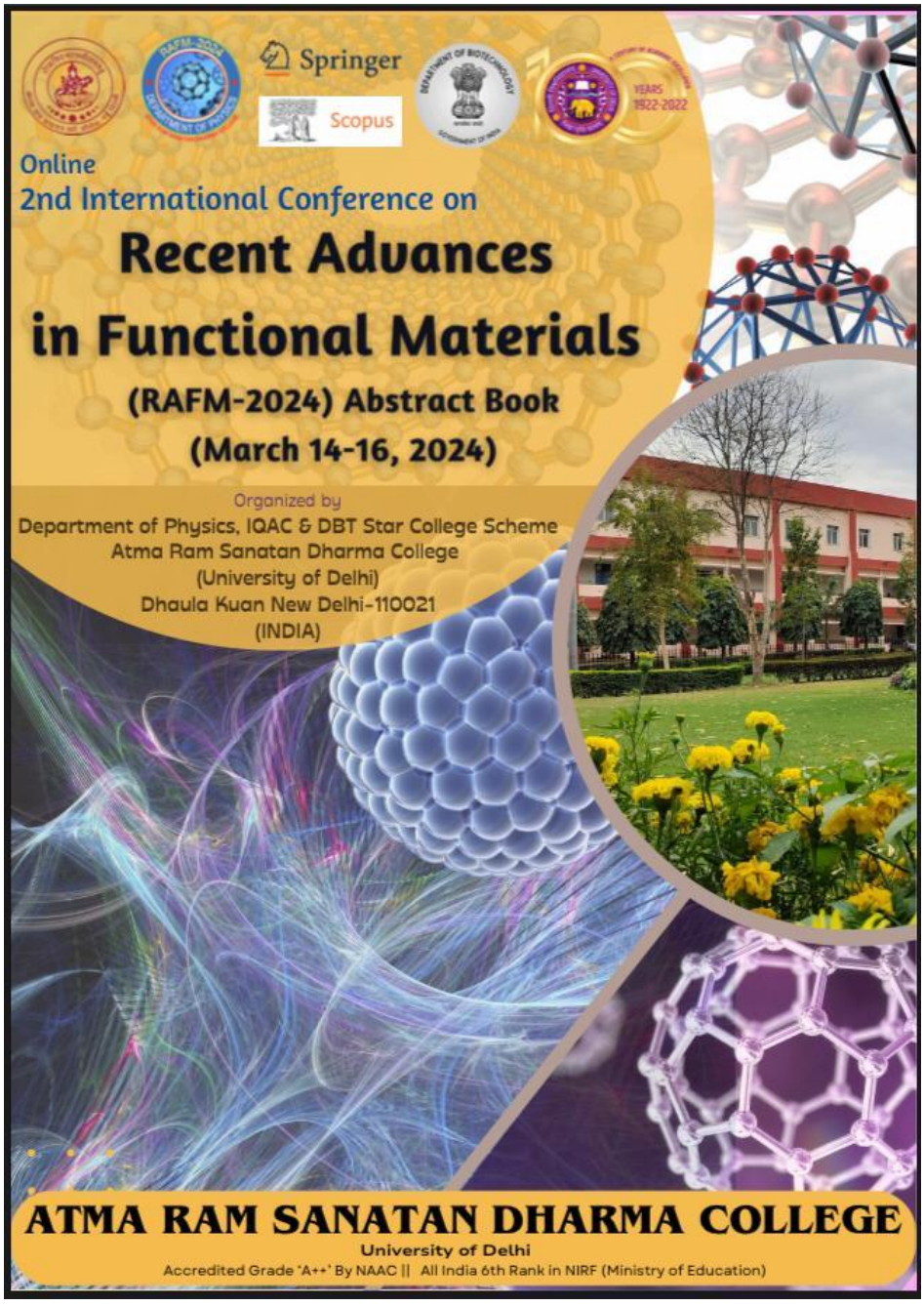

MANUSCRIPT SUBMITTION DETAIL

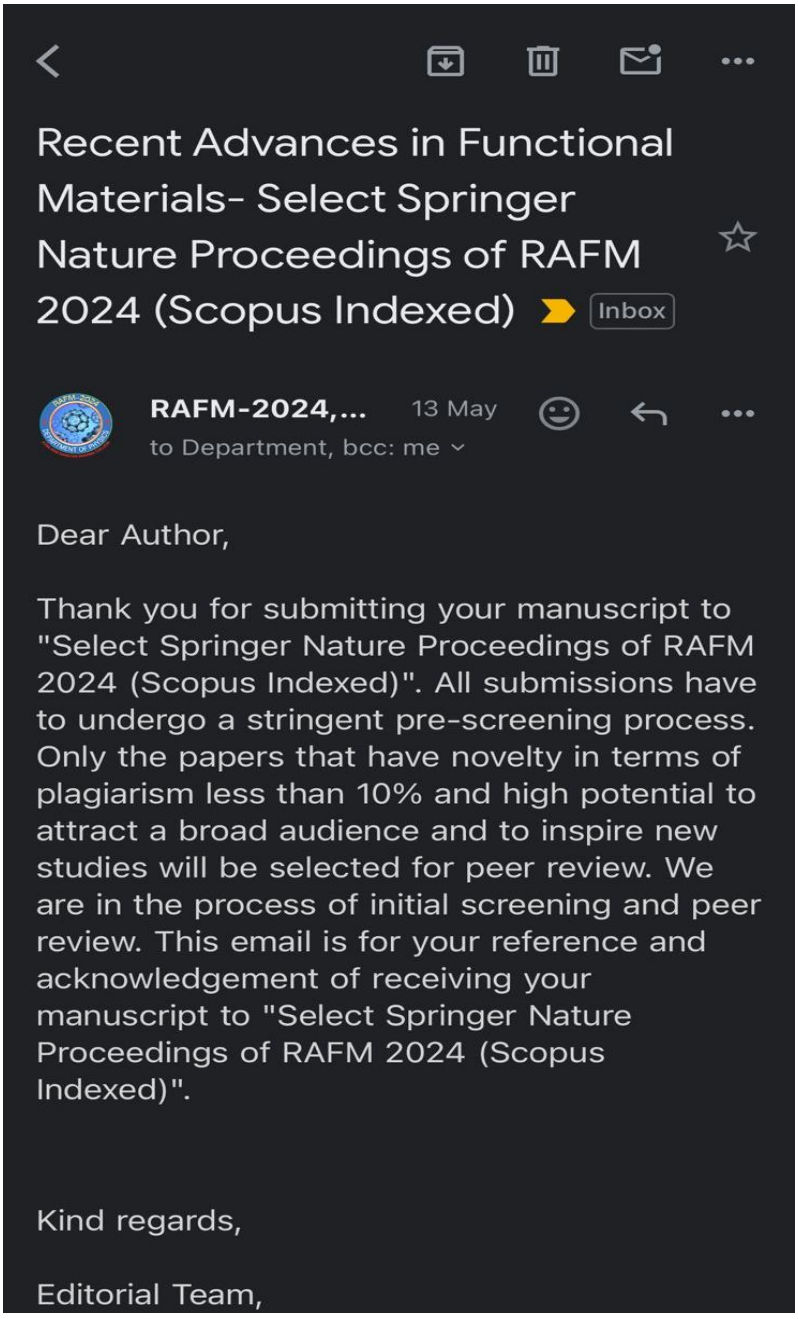

Recent Advances in Functional Materials- Select Springer Nature Proceedings of RAFM 2024 (Scopus Indexed) Inbox

RAFM-2024,... 13 May
to Department, bcc: me

Dear Author,

Thank you for submitting your manuscript to "Select Springer Nature Proceedings of RAFM 2024 (Scopus Indexed)". All submissions have to undergo a stringent pre-screening process. Only the papers that have novelty in terms of plagiarism less than 10% and high potential to attract a broad audience and to inspire new studies will be selected for peer review. We are in the process of initial screening and peer review. This email is for your reference and acknowledgement of receiving your manuscript to "Select Springer Nature Proceedings of RAFM 2024 (Scopus Indexed)".

Kind regards,

Editorial Team,

PLAGIARISM REPORT

Similarity Report

PAPER NAME

Content_Thesis.pdf

WORD COUNT	CHARACTER COUNT
4849 Words	**26466 Characters**
PAGE COUNT	FILE SIZE
21 Pages	**824.4KB**
SUBMISSION DATE	REPORT DATE
Jun 5, 2024 10:49 AM GMT+5:30	**Jun 5, 2024 10:49 AM GMT+5:30**

7% Overall Similarity

The combined total of all matches, including overlapping sources, for each database.

- 4% Internet database
- 3% Publications database
- Crossref database
- Crossref Posted Content database
- 5% Submitted Works database

Excluded from Similarity Report

- Bibliographic material
- Small Matches (Less then 10 words)